

SKELETAL ISOMERISATION ON SULFATED ZIRCONIA MODIFIED BY Ce^{IV} AND Sn^{IV} CATIONS

Mihaiela Ropot^{*}, Ruxandra Barjega^{**}, Floreta Constantinescu^{***}

abstract: Sulfated zirconia and modified sulfated zirconia $Zr_{0.85}Me^{IV}_{0.15}O_2/SO_4^{2-}$ ($M = Ce^{IV}$, Sn^{IV}) have been studied as catalysts for skeletal isomerisation of n-butane. The correlation between the structure, porosity, the solid-acid character of these samples and their catalytic performances were reported.

key words: Modified sulfated zirconia; n-butane isomerisation.

Introduction

Sulfated metal oxides, particularly sulfated zirconia have been widely studied in the past 20 years because they present catalytic properties for various carbenium ion type reaction such as the skeletal isomerisation of lower alkanes at low temperature [1-5].

Many studies have been devoted to the investigation of the influence of preparation and of the nature of precursors, on the structural properties and the catalytic performances of sulfated zirconia, which were claimed to have superacidic properties [6-7]. Now it is accepted that this catalyst is not a superacid solid but is merely a strong solid acid; it was shown that its acid sites are not stronger than the Brönsted sites in promoted zeolites and the Lewis sites in γ -Al₂O₃ [8,9].

Different promoted sulfated zirconia with Fe, Co, Cr, W, Ni, Pt or with different oxides such as Al, Ce, Ga, In, Tl, Mo, W were also used as active contact masses in skeletal isomerisation of n-butane [10]. Many studies have come to the conclusion that the skeletal isomerisation of lower alkanes occurs via a bimolecular mechanism while for those with more than five carbons a monomolecular mechanism would be involved [11].

In both cases, however, the dehydrogenation function related to the redox character of the catalyst seems to be important.

The aim of this paper is to prepare high-dispersed composites $Zr_{0.85}Me^{IV}_{0.15}O_2/SO_4^{2-}$ ($M = Ce^{IV}$, Sn^{IV}) and to study the promoting effect of these sulfated zirconia catalysts in the skeletal isomerisation of n-butane. The presence of the modified cations in the zirconia

* University of Bucharest, Faculty of Chemistry, 4-14 Regina Elisabeta, Bucharest 3, 70346, Romania

** S.C. ZECASIN S.A., 202 Splaiul Independentei, Bucharest, Romania

*** SNP – PETROM, Research Institute for Petroleum Processing and Petrochemistry, 291 A, Republicii Blvd., Ploiesti 2000, Romania

lattice may induce the changes in the concentration and strength of acid sites and also in the redox ability of these catalysts. The correlation between the structural, the acid properties of the catalysts and their catalytic performances are also discussed.

Experimental

Catalysts preparation.

The $Zr(OH)_4$ and $Zr_{0.85}Me_{0.15}^{IV}(OH)_4$ were obtained by hydrolysis of ethanol solutions of $ZrCl_4$ and admixture of this compound and $Ce_2(NO_3)_2 \cdot 6H_2O$ or $SnCl_4$; these solutions were dropped under vigorous stirring, at room temperature in an aqueous hydrazine hydrate 20 % (w/w) solution. During the precipitation the pH remained 9. The precipitates were maturated 72 hours at 60 °C, the pH being unchanged. Then the product was filtered and washed with distilled water to remove all chlorine ions. Finally the gels were dried for 12 hours at 110 °C. Sulfated samples were prepared by impregnation of the dried gels for 24 hours with a 1N H_2SO_4 solution (15 ml/g of hydrous zirconium oxides), followed by filtration and drying at 110 °C for 12 hours. The solids were calcinated in an air stream (20 $cm^3/min.$) at 600 °C for 2 hours.

Catalysts characterization.

Differential thermal analysis were carried out on dried $Zr(OH)_4$ and $Zr_{0.85}Me_{0.15}(OH)_4$ and also on the sulfated samples. Both TG/DTA data were obtained simultaneous at a heating rate of 10 °C/min by using MOM-Q 1500 D equipment. The specific surface areas of the catalysts were determined by nitrogen adsorption isotherms at liquid nitrogen temperature, using a BET and Dubinin-Raduskyedici equations. The sulfated samples were examined by X-ray diffraction (XRD) using a Ni-filtered $CuK\alpha$ radiation with a goniometer speed of 1 °C/min. from 10 °C to 80 °C. For quantitative analysis a step scanning technique was applied in the 2θ range of 27-37°, with a step of 0.02° for 20 s. at each step. SiO_2 - α -quartz was used as internal standard. The acidity of the samples was measured by ammonia TPD in the range of 100-500 °C.

The experiments were carried out in conventional equipment using a quartz microreactor, at the heating rate of 10 °C/min. in nitrogen flow; the microreactor was coupled at a GL chromatograph with TC detector. Catalytic tests were performed in a quartz microflow reactor with fixed bed at atmospheric pressure using 0.5 g of catalyst (0.4-0.5 mm fraction). The reactant flow was an admixture of argon and n-butane in a molar ratio 2:1. $W/F = 16.8$ mol $n-C_4H_{10} \cdot g_{cat} \cdot h^{-1}$ was used. On-line analysis of the products was made in a ThermoQuest Trace GC 2000 Gas Chromatography with FID detector and a capillary column with stationary phase GS-Alumina, 30m x 0.53 mm I.D.

Results and discussion

Thermogravimetric results are shown in the table 1.

Table 1. TG/DTA results for unsulfated and sulfated samples

Sample	Exothermic peak (°C)	Total weight loss (wt %)	Q ^a (u.c)
Zr(OH) ₄	420	1.68	3.11
Zr(OH) ₄ /SO ₄ ²⁻	615	3.72	3.60
Zr _{0.85} Ce _{0.15} (OH) ₄	380	3.77	5.95
Zr _{0.85} Ce _{0.15} (OH) ₄ /SO ₄ ²⁻	600	1.73	3.59
Zr _{0.85} Sn _{0.15} (OH) ₄	430	4.35	7.92
Zr _{0.85} Sn _{0.15} (OH) ₄ /SO ₄ ²⁻	600	3.80	7.69

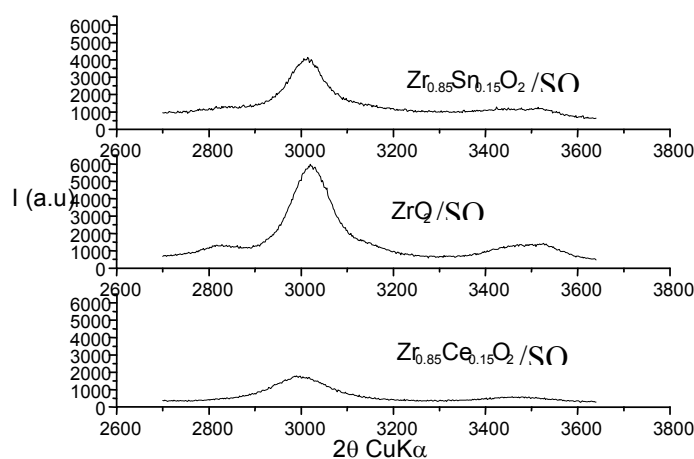
^a Crystallization surface effect/g dehydrated sample

The catalytic precursor samples Zr(OH)₄ or Zr_{0.85}Me^{IV}_{0.15}(OH)₄ exhibit, between 130-330 °C, a wide and intensive endothermic peak assigned to the loss of hydration and constitution water. The hydrous oxides show an intensive exothermic peak at 380-420 °C, which is likely, related to the crystallization of ZrO₂. For the sulfated samples, the exothermic peak is shifted to a higher temperature; this is wider and of much lower intensity. These results seem to be possible that M^{IV} ions are substituted in the ZrO₂ lattice. Over 600 °C the TG curve indicates a small but continuous weight loss of sample corresponding to the partial decomposition of the sulfate groups. At 850 °C another exothermic peak of lower intensity suggested that a change of crystalline structure. The surface area of sulfated zirconia and sulfated-doped zirconia samples are shown in table 2.

Table 2. Surface area and sulfur content of the sulfated zirconia catalysts.

Sample ^a	Surface area (m ² /g)	Pore volume 0-300 Å (cm ³ /g)	Pore volume 0-100 Å (cm ³ /g)	Sulfur content (wt %)
ZrO ₂ /SO ₄ ²⁻	110	0.1864	0.1715	2.23
Zr _{0.85} Ce _{0.15} O ₂ /SO ₄ ²⁻	107	0.1343	0.1222	2.08
Zr _{0.85} Sn _{0.15} O ₂ /SO ₄ ²⁻	126	0.1905	0.1657	2.64

^a calcinated at 600 °C for 2 hours.

**Fig. 1. XRD patterns of the samples in the 2θ range 27-37°.**

All the catalysts present a high surface area and the pore volume distribution indicates that the adsorbents possess a well-defined mesopore structure with a maximum corresponding to pores with 50-75 Å diameter. XRD patterns of the sulfated samples are presented in the figure 1.

The volume fraction of the tetragonal phase could be determined from the empirical formula of Porter and Heuer [12] or using a similar empirical equation proposed by Toraya et al. [13]

The results presented in table 3. are similar, the differences might be accounted to the low monoclinic phase content.

Table 3. The content of the tetragonal phase of the samples and their lattice parameters of the main tetragonal phase.

Samples	V _t (%) [2]	V _t (%) [3]	a(Å)	c(Å)	c/a	V(Å ³)	D* (Å)
ZrO ₂ /SO ₄ ²⁻	86	81	5.09	5.20	1.022	134.5	85
Zr _{0.85} Sn _{0.15} O ₂ /SO ₄ ²⁻	91	86	5.10	5.22	1.024	135.9	90
Zr _{0.85} Ce _{0.15} O ₂ /SO ₄ ²⁻	100	100	5.14	5.21	1.015	137.7	54

* D is the average crystallite size along (1,1,1) direction calculated by Sherrer's formula $D=0.91\lambda/(\beta\cos\theta)$ where λ is the wavelength (Cu K α), β the correct half-width obtained using α -quartz as reference and the Warren formula and θ the diffraction angle [8].

The volume fraction of the tetragonal phase were correlated with the values of the temperatures for the exothermic peak from DTA profiles which increased with the percentage of the volume of the tetragonal phase as a result of the stabilizing role played by the cationic doping, explained partially by a bulk free energy effect.

As figure 1 shows, it should be pointed out that, for the Zr_{0.85}Ce_{0.15}O₂/SO₄²⁻ sample, because of the line broadening due to the fine crystallite size, some uncertainties in discriminating between the tetragonal (*t*) and the cubic (*c*) - phases subsist. However, as the full-width at half-maximum (half-width) of the $2\theta = 34.69^\circ$ is considerably larger the half-width of the $2\theta = 29.98^\circ$ we should assume that the $2\theta = 34.69^\circ$ peak is actually, the convolution of the 0,0,2 and 2,0,0 tetragonal peaks. The fitting of the profiles reveals improved standard fitting errors by assuming a tetragonal symmetry in stand of a cubic one. It is to be emphasised that for this sample the axial *c/a* ratio of the unit cell is the lowest one, quite close to the unit, revealing that for the ceria-zirconia sample the tetragonal phase has the lowest oxygen displacements from the ideal fluorite positions [14] as a result of the stabilising role played by cerium in the structure. In fact it has been reported [15,16] for zirconia-ceria materials with ceria amounts > 50% XRD patterns with a cubic structure and a lattice parameter moving as the cerium amount increases towards the lattice parameter of the fluorite-type structure of CeO₂.

Table 3 shows some interesting results. Sample Zr_{0.85}Ce_{0.15}O₂/SO₄²⁻ has the largest lattice volume as a result of the Ce⁴⁺ incorporation in the framework (larger ionic radius in comparison with Zr⁴⁺, 1.01Å versus 0.80Å). The lowest axial ratio along with the lowest crystallite size for the ceria-zirconia sample is a clear mark of a stabilised tetragonal phase. For the Zr_{0.85}Sn_{0.15}O₂/SO₄²⁻ one expected the lowest volume as the ionic radius are lowest one (0.71 Å). For this sample an overlapping effect occurred in connection with the transition of the tetragonal phase to the monoclinic phase. This sample has the largest crystallites size and the largest axial ratio too, indicating a higher transformability of the

tetragonal to the monoclinic phase. A crystallite effect size is reported in the literature [14, 17].

Table 4 contains the correlation between the X-ray crystallite size, the BET surface areas and levels of the X-ray background as a measure of the X-ray amorphous material content.

We calculated the surface area derived from the average crystallite size, D (m), determined by XRD, assuming a spherical particle:

$$A_{XRD}[m^2 / g] = 6/(\rho D) \quad (1)$$

where ρ [gm^{-3}] is the density of the crystallite, which we evaluated also as an X-ray density using the crystallographic data and the chemical compositions already determined.

In the evaluation of the background in the 2θ range 27-37° a correction was applied which takes into account the differences in the mass absorption coefficients μ for the $Cu_{k\alpha}$ wavelength. The background level estimated as a constant will ascertain for the differences of the amorphous and very fine crystallites content of these samples.

Table 4. The correlation between the XR crystallite size, the BET surface areas and levels of the XR background.

Sample	$A_{XRD}(m^2.g^{-1})$	$A_{BET}(m^2.g^{-1})$	Background level (a.u)
ZrO ₂ /SO ₄ ²⁻	78	110	620
Zr _{0.85} Sn _{0.15} O ₂ /SO ₄ ²⁻	71	126	827
Zr _{0.85} Ce _{0.15} O ₂ /SO ₄ ²⁻	116	107	382

The results from table 4 lead to the following observation:

- only for the ceria-zirconia sample the BET surface area and XRD area are in good agreement. This result is consistent with the low amorphous amount and the formation only of a pure tetragonal phase for this sample.
- there is a linear correlation between the BET area and the background level attesting for the connection between the amorphous or very fine particles amount and the BET areas.
- the appearance of a larger amounts of an amorphous material is due to the transition from the tetragonal phase to a monoclinic phase accompanied by a volume expansion.
- the highest BET area along with the largest amorphous amount for Zr_{0.85}Sn_{0.15}O₂/SO₄²⁻ is suggested by a larger unit cell volume than for the zirconia sample and the largest crystallites sizes, too. For larger crystallites it seems, that is a higher probability to contain embryonic nuclei which, when they reached a critical size, favour the transition to a monoclinic phase

Temperature-programmed desorption of ammonia has been used as a measure of total acidity and acid strength distribution in solids. The results are shown in table 5.

Table 5. Acidity and acid strength distribution of the catalysts.

Sample	Total acidity (100 °C) mmol NH ₃ ·g ⁻¹	Desorbed NH ₃ mequiv. NH ₃ ·g ⁻¹			Number of strong acid sites/g _{cat}
		Weak acid sites 100-175°C	Medium acid sites 175-300°C	Strong acid sites 300-500°C	
ZrO ₂ /SO ₄ ²⁻	0.70	0.11	0.24	0.35	2.11·10 ²⁰
Zr _{0.85} Sn _{0.15} O ₂ /SO ₄ ²⁻	0.76	0.14	0.29	0.33	1.99·10 ²⁰
Zr _{0.85} Ce _{0.15} O ₂ /SO ₄ ²⁻	0.53	0.17	0.20	0.16	9.64·10 ¹⁹

The ZrO₂/SO₄²⁻ and respectively Zr_{0.85}Sn_{0.15}O₂/SO₄²⁻ samples have the same concentration of strong acid sites even the last one has a greater amount of the weak and medium acid sites. The Zr_{0.85}Ce_{0.15}O₂/SO₄²⁻ sample exhibits a lower total acidity and also a lower concentration of strong acid sites.

The figure 2 shows the variation of the catalytic performances of unpromoted ZrO₂/SO₄²⁻ at different temperature of reaction. The increase of the reaction temperature corresponds to a high activity, which is associated to a lower selectivity.

The activity of sulfated zirconia and promoted samples decreases during the first 30 minutes then it trends to a constant value. (Figure 3). The decrease of catalytic activity in time is due to the fact that by-products are formed as result of the simultaneous secondary reactions, mainly at higher temperature, responsible for their catalytic deactivation. This can also show from the results give in the table 6.

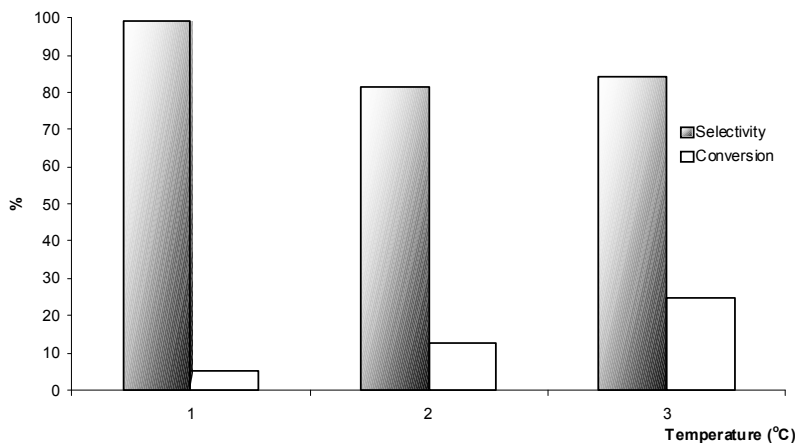


Figure 2. Conversion and selectivity for ZrO₂/SO₄²⁻ at different temperatures. (1): 100°C, (2):150°C, (3) 250°C.

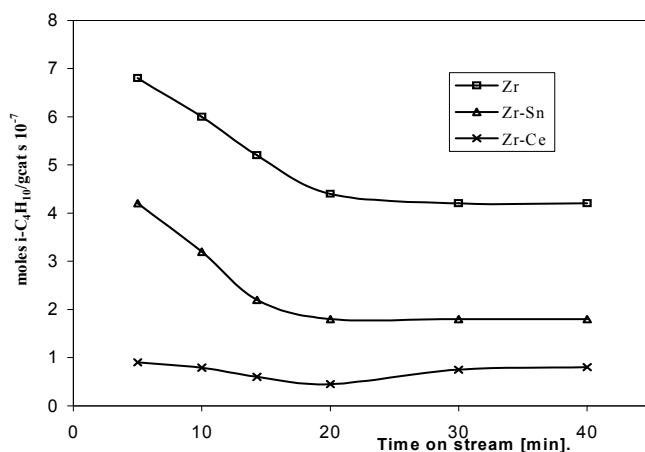


Fig. 3. The activity of sulfated zirconia at 250 °C.
0,5 g catalysts; reactant flow = 5 ml/min.; Ar/n-C₄H₁₀ = 2/1 molar ratio

Table 6. The activity of the catalysts in the skeletal isomerisation of n-butane; temp. = 250°C, 0.5 g catalyst; reactant flow = 5 ml/min, Ar/n-C₄H₁₀ = 2/1 molar ratio;

Sample	Time on stream [min.]	wt %					Conversion n-C ₄ H ₁₀ (%)	Selectivity iso-C ₄ H ₁₀ (%)
		C ₂ +C ₃	iso C ₄ H ₁₀	n-C ₄ H ₁₀	C ₄ H ₈	C ₄ ⁺		
SZ	5	4.72	28.76	57.14	6.06	3.32	42.86	67.10
	30	2.61	18.83	74.58	2.75	1.23	25.42	74.07
SZ-Sn	5	1.20	15.26	81.55	1.59	0.40	18.45	82.71
	30	0.46	8.20	90.60	0.52	0.22	9.40	87.23
SZ-Ce	5	0.61	6.24	92.49	0.46	0.20	7.51	83.08
	30	0.18	3.62	95.83	0.24	0.13	4.17	86.81

*SZ = ZrO₂/SO₄²⁻; SZ-Sn = Zr_{0.85}Sn_{0.15}O₂/SO₄²⁻; SZ-Ce = Zr_{0.85}Ce_{0.15}O₂/SO₄²⁻

Even the activity of promoted catalysts is lesser than for unpromoted ones, the isobutane selectivity is higher for the samples modified by Ce⁴⁺ and Sn⁴⁺. The cracking effect of ZrO₂/SO₄²⁻ is diminished in the same way as the dehydrogenation effect. There have been given for the formation of Zr³⁺ species located on the crystallite surfaces by decomposition of some sulfate groups during the calcination of the catalysts. The redox properties of the catalysts may strongly depend on the surface concentration of these ions having a lower oxidation state. Doping the ZrO₂/SO₄²⁻ lattice with different tetravalent ions, which can also change their oxidation state, we are able to discreetly modify the redox properties of these catalysts. The correlation of these results shown that the doping of zirconia lattice with Ce⁴⁺ and respectively Sn⁴⁺ ions has as effect the stabilization of the tetragonal phase, an increase of the surface area and the modification of the crystallite dimensions. The catalytic activity depends on both, the concentration of the strong acid sites and the electron acceptance ability of the solid as a result of the enhancement of the redox properties. The presence of Sn⁴⁺ ions seem to modified the redox sites population without affecting essentially the acidity of the solid, which has a lower activity than unpromoted sulfated zirconia but higher selectivity in isobutane formation. As already was shown the first step of reaction implies the abstraction of hydrogen from hydrocarbon substrate and for this purpose the acid sites as well as the redox properties of the catalyst are manly responsible. This step is the cause

of the activity of these catalysts and also of their deactivation, because dehydrogenated species lead to polymerisation. Even the dehydrogenated function of the promoted catalysts is lower than the unpromoted sample, the doped ions may diminish the polymerisation function and enhance the consumption of olefins by a bimolecular mechanistic pathway of skeletal isomerisation of n-butane.

Conclusions

The preparation of the doped sulfated zirconia by soft chemistry as well described leads to the synthesis of a stable ZrO₂ tetragonal phase; these solids have a particular texture characterised by a pore diameter in the mesoporous range. The synthesised composites Zr_{0.85}Me^{IV}_{0.15}O₂/SO₄²⁻ (M = Ce^{IV}, Ti^{IV}, Sn^{IV}) having the same sulfur content have lower activity than undoped sulfated zirconia, but they are more selective in skeletal isomerisation of n-butane.

REFERENCES

1. Hino M., Kobayashi S. and Arata K., (1979)*J. Am. Chem. Soc.*, **101**, 6439.
2. Hino M. and Arata K., (1980)*J. Chem. Soc., Chem. Commun.*, 851.
3. Arata K., *Adv. Catal.*, (1990), **37**, 165.
4. Tanabe K. and Yamaguchi T. (1990), *Stud. Surf. Sci. Catal.*, **44**, 99.
5. Tanabe K., Hattori H. and Yamaguchi T., (1990) *Crit. Rev. Surf. Chem.*, **1**, 1.
6. P. Moles, *Spec. Chem.*, **12**, 382 (1992).
7. B. H. Davis, R. A. Keogh, R. Srinivasan, *Catal. Today*, **20**, 219 (1994).
8. Yin-Yan Huang, Bi-Ying Zhao, You-Chang Xie, *Appl. Catal.*, **75-83**, 171 (1998).
9. V. Adeeva, J. W. de Hann, J. Janchen, G. D. Lei, V. Schunemann, L.J.M. van de ven, W.M.H. Sachtler, R. A van Santen, *J. Catal.*, **151**, 365 (1995).
10. X. Song, A. Sayari, *Catal. Rev.-Sci. Eng.*, **38(3)**, 329-412 (1996).
11. E. Iglesia, S.L. Soled, G.M. Kramer, *J. Catal.*, **144**, 283 (1993).
12. D.L. Poster and A.H. Heuer, *J. Am. Ceram. Soc.*, **62** [5-6], 298-305 (1968).
13. H. Toraya, M. Yoshimura, S. Somaya, *J. Am. Ceram. Soc.*, **67**, C-119 (1984).
14. W. Stichert and F. Schüth, *Chem. Mater.*, **10**, 2020-2026 (1998).
15. S. Rossignol, Y. Madier, D. Duprez, *Catalysis Today*, **50**, 261-270 (1999).
16. S. Rossignol, F. Gerard and D. Duprez, *J. Mater. Chem.*, **9**, 1615-1620 (1999).
17. R.C. Garvie, *J. Phys. Chem.* **82**, 216-224 (1978).